

RESEARCH AND REVIEWS: JOURNAL OF MATERIAL SCIENCES

Synthesis, Characterization of Nano MnO₂ and its Adsorption Characteristics Over an Azo Dye.

BM Pradeep Kumar^a, Sriram Karikkat^b, R Hari Krishna^c, TH Udayashankara^b, KH Shivaprasada^a, and BM Nagabhushana^{c*}.

^aDepartment of Chemistry, V. S. K. University, Bellary -583105, India.

^bDepartment of Environmental Engineering, Sri Jayachamarajendra College of Engineering, Mysore -570 006, India

^cDepartment of Chemistry, M. S. Ramaiah Institute of Technology, Bangalore 560 054, India.

Research Article

Received: 22/11/2013

Revised: 12/12/2013

Accepted: 19/12/2013

*For Correspondence

Department of Chemistry, M. S. Ramaiah Institute of Technology, Bangalore 560 054, India.

Keywords: Nano MnO₂, Solution combustion, Adsorption, Direct green dye

ABSTRACT

Nano MnO₂ powder was synthesized by low temperature solution combustion method using oxalyl dihydrazide (ODH) fuel. The final product was well characterized by Powder X-ray diffraction (PXRD), Fourier Transform Infrared Spectroscopy (FTIR) and Scanning electron microscopy (SEM) for crystallographic purity, phase formation and surface morphology respectively. PXRD results show that pure MnO₂ was synthesized at 300 °C with no other impurities. SEM micrograph shows the product has highly porous structure with large voids, typical of combustion derived material. An adsorption characteristic of the porous MnO₂ was studied over direct green dye (DG). The optimum dose of MnO₂ for removal of 10 ppm DG azo dye was found to be 0.4 g L⁻¹.

INTRODUCTION

The textile industries are becoming a major source of environmental contamination because an alarming amount of dye pollutants are generated during the dyeing processes^[1]. In fact, about 700000 tonnes of different dyes are produced annually in the world, among which about 50000 tonnes of dyes are discharged into the environment^[2]. Organic dyes are one of the largest pollutants released into wastewater from textile and other industrial processes, which have shown severe impacts on human physiology^[3,4]. Some dyes like azo-dyes and fluorescein dyes have been found to be highly cytotoxic for the mammalian tissues^[5,6]. The organic groups present in dyes result in the formation of certain reactive intermediates, which trigger the morphological and genetic alterations, thereby making the dye cytotoxic and carcinogenic. Synthesis, properties and application potential of semiconductor nanoparticles manifesting photocatalytic activity in various redox-processes have been and the subject of great interest to the present day^[7,8]. In addition several novel adsorbents have been reported to possess great adsorption potential due to their enhanced adsorptive capacity^[9]. Nano-structure compounds have gained importance in this category due their anticipated high surface area and improved reactive sites^[10,11]. Nano-MnO₂ has great potential applications in environment protection field as a new generation of environmental friendly catalyst. There are a number of research results which show that the functional activity of semiconductor materials depends on the structure. Manganese oxide is one of the most interesting materials, which has a wide variety of structure with large surface area. The diverse structures, chemical properties of manganese oxides are taken advantage of in potential applications such as cation-exchange^[12], ion and molecule separation^[13-14], adsorbents^[15], sensor^[16], battery^[17], catalysis^[18] etc. It is also used for a wide catalytic applications, such as degradation of dyes^[19,20], photocatalytic oxidation of organic pollutants and waste water treatment^[21], nitric oxide reduction^[22], ozone decomposition^[23], selective oxidation of CO^[24], alcohols^[18] etc., The diverse chemical properties makes the MnO₂ material unique. MnO₂ with different physical and chemical properties, such as crystallinity, amount of combined water, specific surface areas, and electrochemical performance, can be yielded under different synthesis conditions.

Nanostructured materials become more and more attractive in recent years, because these materials possess favorable and enhanced physical and chemical properties. Much effort has been made toward the preparation of MnO₂ nanostructures with different morphologies^[25,26,27]. However, very few reports on the synthesis of MnO₂ nanostructures with Solution combustion. In this paper, we report a facile, energy saving method to

synthesize MnO₂ nano powders with highly porous structure via solution combustion route and its potential application in removal of organic dye from aqueous solution.

EXPERIMENTAL

Synthesis of nano MnO₂

The synthesis process involved the combustion of redox mixtures in which Manganese nitrate [Mn(NO₃)₂·H₂O] acted as an oxidizing reactant and oxalyl di-hydrazide (ODH) [C₂H₆N₄O₂] as a reducing one. The initial composition of solution containing manganese nitrate and ODH was calculated based on the total oxidizing and reducing valences of the oxidizer and the fuel using the concepts of propellant chemistry^[28]. All the reagents were of analytical purity, and used without further purification. Manganese nitrate and ODH were mixed with minimum quantity of doubled distilled water in a cylindrical petri dish and stirred for few minutes until clear solution is formed. The dish was introduced into a muffle furnace maintained at 300 °C. The solution initially undergoes dehydration, followed by decomposition with the evolution of large amounts of gases. The mixture then froths and swells forming foam, very soon the flames spread the entire volume forming black porous product. The entire combustion process is over in 5 min. The foam was grinded to obtain fine powder of MnO₂.

Instruments used

The PXRD patterns of MnO₂ samples were obtained using a Philips PW/1050/70/76 X-ray diffractometer using CuKα radiation at a scan rate of 2°/min. The morphology of powders was examined using JEOL (JSM-840A) scanning electron microscopy (SEM). FTIR spectra were recorded using Nicollet IMPACT 400 D FTIR spectrometer, in the range 400–4000 cm⁻¹ as KBr pellet. The absorption spectra were recorded with a UV-visible spectrophotometer (Elico-159).

RESULTS AND DISCUSSION

Characterization of nano-catalyst

Powder X-ray diffraction (PXRD)

Figure 1. shows the PXRD pattern of the MnO₂ powder prepared using ODH as fuel in stoichiometric fuel-to-oxidant ratio at 300 °C. The typical PXRD patterns show broad diffraction peaks corresponding to Bragg's reflections from (120), (131), (300), (160) and (003) planes which corresponds to gamma phase MnO₂ (according with JCPDS 14-644) with no other impurity peaks. The crystallite size was estimated using Scherrer's formula given by the relation

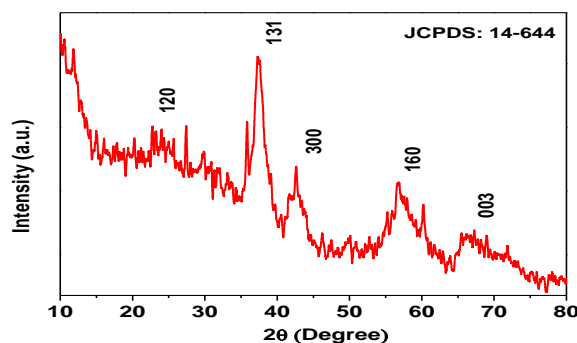


Figure 1: PXRD pattern of MnO₂ nano powder

$$D=0.9\lambda/\beta\cos\theta \quad \dots\dots\dots(i)$$

The crystallite size estimated by this method is found to be in the range 15-20 nm.

Scanning Electron Microscopy (SEM)

SEM micrograph (Fig.2) shows the overall appearance of the combustion derived product. The particles are almost spherical with varying sizes, might be due to non uniform distribution of temperature during combustion. It can be observed that product aggregation is constituted by many irregular particles with a variety of pores and

voids due to the evolution large amount of gases that are formed as by product during synthesis. This type of structure is typical of combustion derived samples. Highly porous nature of MnO_2 facilitates and enhances the adsorption characteristics.

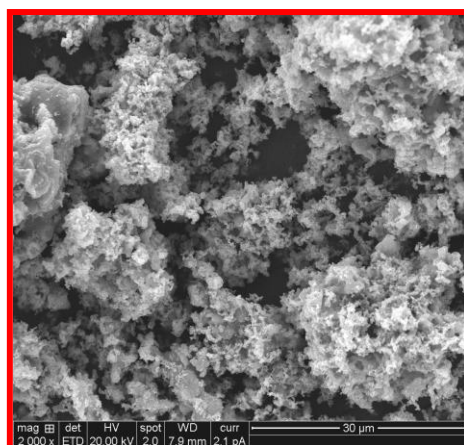


Figure 2: SEM micrograph of nano MnO_2 .

Fourier Transform Infrared Spectrum (FTIR)

The FT-IR spectrum was used to identify the functional groups and other impurities present in the final product. Fig. 3 represents the spectrum of the MnO_2 nano powder prepared by solution combustion method. The broad band at 3438 cm^{-1} is believed to be associated with the stretching vibrations of hydrogen-bonded surface water molecules and hydroxyl groups. Additionally, the bands at 1645 and 1386 cm^{-1} correspond to the existence of large numbers of residual hydroxyl groups, which imply the O-H vibrating mode of traces of adsorbed water. The band located at 539 cm^{-1} can be ascribed to the Mn-O vibrations of MnO_2 nano powder. The FTIR analysis presented here is consistent with the results reported in the literatures^[29, 30].

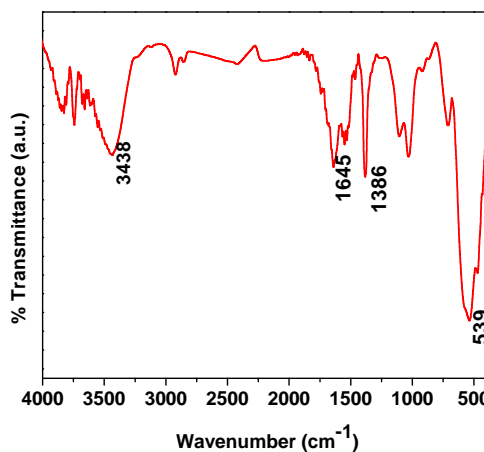


Figure. 3. FTIR spectra of MnO_2 nanopowder

ADSORPTION ACTIVITY OF NANO MnO_2 OVER DIRECT GREEN DYE

Direct green dye has a molecular formula of $\text{C}_{34}\text{H}_{22}\text{N}_8\text{Na}_2\text{O}_{10}\text{S}_2$ and its molecular weight of 767.7. Direct dyes colour cellulose fibres directly without the use of mordant. They are used for dyeing wool, silk, nylon, cotton, rayon etc. Direct dyes colour cellulose fibres directly without the use of mordant. It has a strong, though apparently non-covalent affinity to cellulose fibres. However, its tendency to change colour when touched by sweaty fingers and its toxicity has proven to be a disadvantage to its best use.

In order to evaluate adsorption activity of the combustion derived MnO_2 sample, batch adsorption studies of direct green dye was done. A typical experiment constitutes 50 ml of 10 ppm dye solution and different amount of adsorbent were taken in a glass reactor. The mixture was stirred in dark for 30 minutes to establish the

adsorption equilibrium between the dye molecules and the catalyst surface. The decolourization efficiency (%) was calculated as follows

$$\% \text{ Removal} = C_0 - C / C_0 \times 100 \dots (ii)$$

Where C_0 is the initial concentration of dye and C is the concentration of dye after adsorption.

Effect of MnO_2 dose

Experiments were carried out using different amounts of MnO_2 , keeping dye concentration constant at 10 ppm [Fig. 4]. It was found that the adsorption increases up to 20 mg/50 ml of the dye solution, beyond which it shows a sudden reduction. The increase in the adsorption efficiency of DG with increase in the amount of adsorbent may be due to increase in the active sites available on the adsorbent. Decrease in adsorption beyond 20 mg is due to desorption of dye due to increased collisions between adsorbent. The percentage removal of DG is about around 67 % at neutral pH for 30 min contact time.

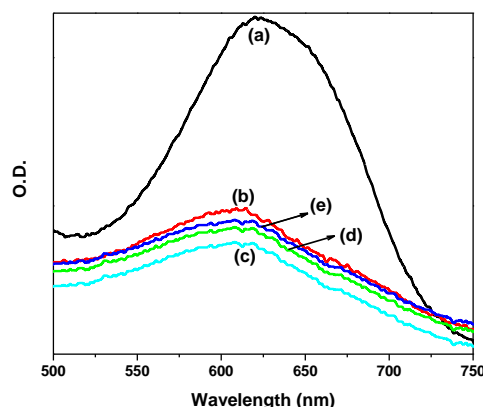


Figure 4: UV-Vis spectra of (a) blank DG dye (b) 10 mg MnO_2 (c) 20 mg MnO_2 (d) 30 mg MnO_2 (e) 40 mg MnO_2 .

CONCLUSIONS

In this study, highly porous and crystalline nano MnO_2 was synthesized by low temperature combustion synthesis. The adsorbent consists of monocrystalline particles of 15-20 nm size. The ability of MnO_2 to adsorb DG was investigated by batch adsorption studies. The amount of dye adsorbed was found to vary with adsorbent dosage. The amount of dye uptake (mg/g) was found to increase with increase in adsorbent dose upto 0.4 g L^{-1} and beyond which it decreases. It can be concluded that the combustion derived nano porous MnO_2 is an efficient adsorbent for the removal of DG from aqueous solution.

REFERENCES

1. WC Tincher. Enhanced Rates of Photocatalytic Degradation of an Azo Dye Using SnO_2/TiO_2 Coupled Semiconductor Thin Films. *Text Chem Color*. 1989; 21: 33.
2. RS Blackburn. Natural Polysaccharides and Their Interactions with Dye Molecules: Applications in Effluent Treatment. *Environ Sci Technol*. 2004; 38: 4905.
3. A Panandikar, C Fernandes, VKV Rao. The cytotoxic properties malachite green are associated with increased demethylase, aryl hydrocarbon hydrolase and lipid peroxidation in primary cultures of syrian hamster embryo cells. *Cancer Lett*. 1992;67: 93.
4. A Panandikar, GB Maru, VKV Rao. Dose-response effects of malachite green in free radical formation, lipid peroxidation and DNA damage in Syrian hamster embryo cells and their modulation by antioxidants. *Carcinogenesis*. 1994; 15: 2445.
5. CR Nony, MC Bowman. Metabolism studies of an azo dye and pigment in the hamster based on analysis of the urine for potentially carcinogenic aromatic amine metabolites. *T Cairns J Anal Toxicol*. 1980: 4:132.
6. RB Haveland-Smith, RD Combes, BA Briges. Studies on the genotoxicity of some fluorescein dyes. *Mutat Res*. 1981; 88: 1.
7. A Pourahmad, Sh Sohrabnezhad, E Kashefian. AgBr/nano AIMCM-41 visible light photocatalyst for degradation of methylene blue dye. *Spectrochim Acta Part A*. 2010; 77: 1108.
8. A Pourahmad, Sh Sohrabnezhad, E Radaee. Degradation of Basic Blue 9 dye by CoS/nanoAIMCM-41 catalyst under visible light irradiation. *Porous Mater*. 2010; 17: 367.

9. QU Jiuhui. Research progress of novel adsorption processes in water purification: a review. *J Environ Sci.* 2008; 20: 1.
10. R Nagaraja, B Nagappa, CR Girija, BM Nagabhusana. Synthesis and Characterization of Nanocrystalline MgO Powder and its Application in the Treatment of Pharmaceutical Effluent. *J Nanotech Appl.*, 2011; 11: 28.
11. Stark JV. et al. Nanoscale Metal Oxide Particles/Clusters as Chemical Reagents. Unique Surface Chemistry on Magnesium Oxide As Shown by Enhanced Adsorption of Acid Gases (Sulfur Dioxide and Carbon Dioxide) and Pressure Dependence. *Chem Mats.* 1996: 81: 1904.
12. Q Feng, H Kanoh, K Ooi. Manganese oxide porous crystals. *J Mater Chem.* 1999;9:319
13. Oscar Giraldo, Stephanie L. Brock, William S. Willis, Manuel Marquez, Steven L. Suib. Manganese Oxide Thin Films with Fast Ion-Exchange Properties. *J Am Chem Soc.* 2000;122(38):9330-9331
14. YF Shen, et al. Manganese Oxide Octahedral Molecular Sieves: Preparation, Characterization, and Applications. *Sci.* 1993;11: 260
15. LA Attar, A Dyer. Sorption behaviour of uranium on birnessite, a layered manganese oxide. *J Mater Chem.* 2002; 12: 1381
16. YH Bai, Y Du, JJ Xu, HY Chen. Choline biosensors based on a bi-electrocatalytic property of MnO₂ nanoparticles modified electrodes to H₂O₂. *Electrochem Commun.* 2007; 9: 2611
17. M Nakayama, T Kanaya, JW Lee, BN Popov. Electrochemical synthesis of birnessite-type layered manganese oxides for rechargeable lithium batteries. *J Power Sources.* 2008; 179: 361
18. X Shen, Y Ding, J Liu, K Laubernds. Synthesis, Characterization, and Catalytic Applications of Manganese Oxide Octahedral Molecular Sieve (OMS) Nanowires with a 2 × 3 Tunnel Structure. *Chem Mater.* 2004;16: 5327
19. SR Segal, SL Suib, L Foland. Decomposition of Pinacyanol Chloride Dye Using Several Manganese Oxide Catalysts. *Chem Mater.* 1997; 9: 2526
20. W Zhang, Z Yang, X Wang, Y Zhang, X Wen, S Yang. Large-scale synthesis of β-MnO₂ nanorods and their rapid and efficient catalytic oxidation of methylene blue dye. *Catal Commun.* 2006; 7: 408
21. J Chen, JC Lin, V Purohit, MB Cutlip, SL Suib. Photoassisted catalytic oxidation of alcohols and halogenated hydrocarbons with amorphous manganese oxides. *Catal Today.* 1997; 33: 205
22. L Chen, T Horiiuchi, T Mori. Catalytic reduction of NO over a mechanical mixture of NiGa₂O₄ spinel with manganese oxide: influence of catalyst preparation method. *Appl Catal A.* 2001; 209: 97
23. R Rahakrishnan, ST Oyama. Ozone Decomposition over Manganese Oxide Supported on ZrO₂ and TiO₂: A Kinetic Study Using in Situ Laser Raman Spectroscopy. *J Catal.* 2001;199:282
24. GG Xia, YG Yin, WS Willis, JY Wang, SL Suib. Efficient Stable Catalysts for Low Temperature Carbon Monoxide Oxidation. *J Catal.* 1999;185: 91
25. M Toupin, T Brousse, D Belanger. Influence of microstructure on the charge storage properties of chemically synthesized manganese dioxide. *Chem Mater.* 2002;14: 3946.
26. D Zheng, et al. One-step preparation of single-crystalline beta-MnO₂ nanotubes. *J Phys Chem B.* 2005; 109: 16439
27. V Subramanian, HW Zhu, R Vajtai, PM Ajayan, BQ Wei. Hydrothermal synthesis and pseudocapacitance properties of MnO₂ nanostructures. *J Phys Chem B.* 2005;109: 20207
28. S Ekambaram, N Arul Dhas, KC Patil. Synthesis and properties of aluminium borate (a light-weight ceramic). *Int J Self-prop High-temp. Synth.* 1995; 4: 85
29. XJ Yang, et al. Structural Characterization of Self-Assembled MnO₂ Nanosheets from Birnessite Manganese Oxide Single Crystals. *Chem Mater.* 2004; 16: 5581
30. R Yang, Z Wang, L Dai, L Chen. Synthesis and characterization of single-crystalline nanorods of α-MnO₂ and γ-MnOOH. *Mater Chem Phys.* 2005;93: 149